Pulsars

1967, Cambridge

S. Jocelyn Bell Burnell

Nature 217, 709-713 (24 February 1968)

Observation of a Rapidly Pulsating Radio Source

A. HEWISH, S. J. BELL, J. D. H. PILKINGTON, P. F. SCOTT & R. A. COLLINS

1. Mullard Radio Astronomy Observatory, Cavendish Laboratory, University of Cambridge

Abstract

Unusual signals from pulsating radio sources have been recorded at the Mullard Radio Astronomy Observatory. The radiation seems to come from local objects within the galaxy, and may be associated with oscillations of white dwarf or neutron stars.

In Google: about 16400000 results for **pulsar**

THE DISCOVERY OF THE BINARY PULSAR

Nobel Lecture, December 8, 1993

by RUSSELL A. HULSE

Princeton University, Plasma Physics Laboratory, Princeton, NJ 08543, USA

Pulsars were first discovered in 1967 by Antony Hewish and Jocelyn Bell at Cambridge University, work for which a Nobel Prize was awarded in 1974.

At the time, they were engaged in a study of the rapid fluctuations of signals from astrophysical radio sources known as scintillations. They were certainly not expecting to discover an entirely new class of astrophysical objects, just as we were certainly not expecting to discover an astrophysical laboratory for testing general relativity when we started our pulsar search at Arecibo several years later. Pulsars have indeed proven to be remarkable objects, not the least for having yielded two exciting scientific stories which began with serendipity and ended with a Nobel Prize.

Pulsar distribution

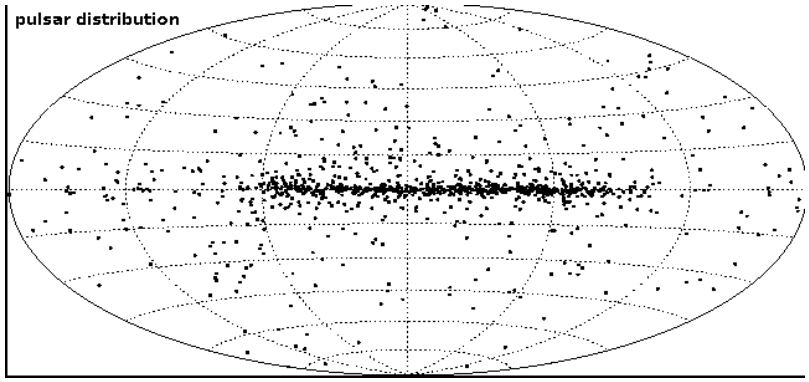

in galactic coordinates

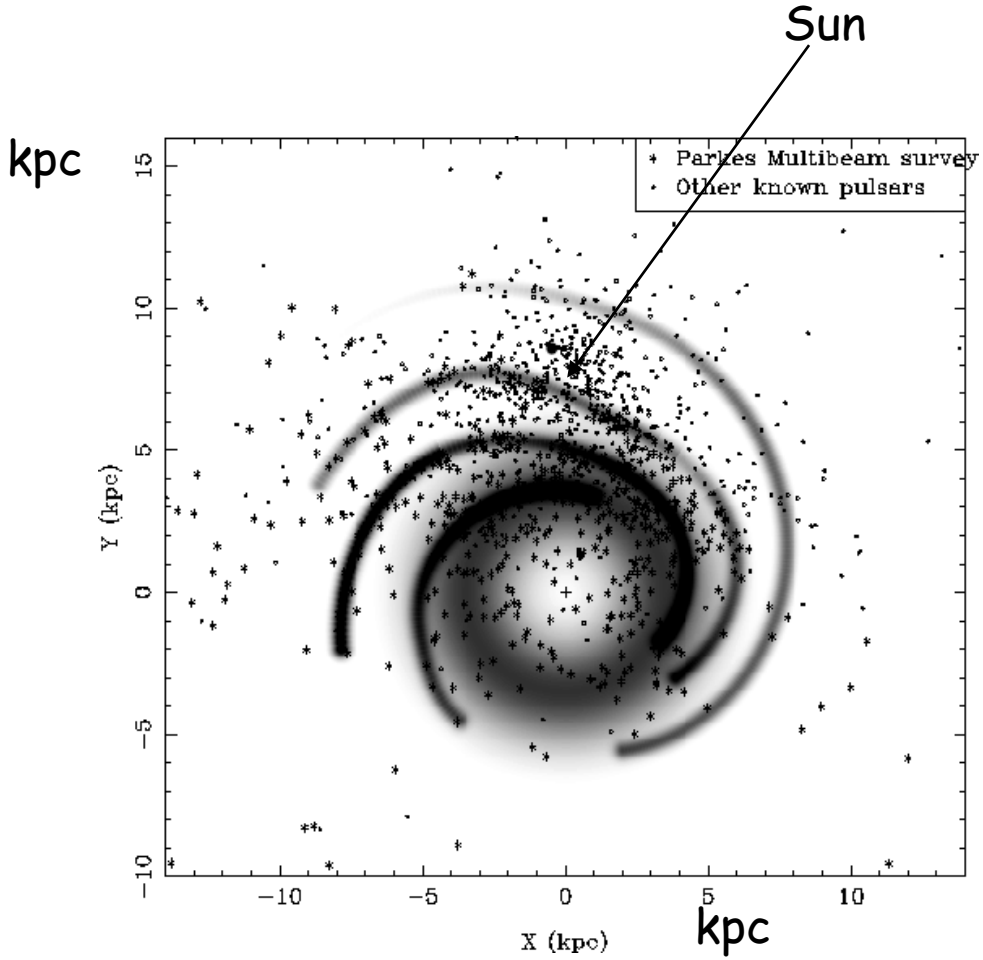

+ galactic centre

Distribution of interstellar free electrons model in grey scale

Pulse profile

For a pulsar:

Differences in the profile from pulse to pulse

Integrated profiles very stable

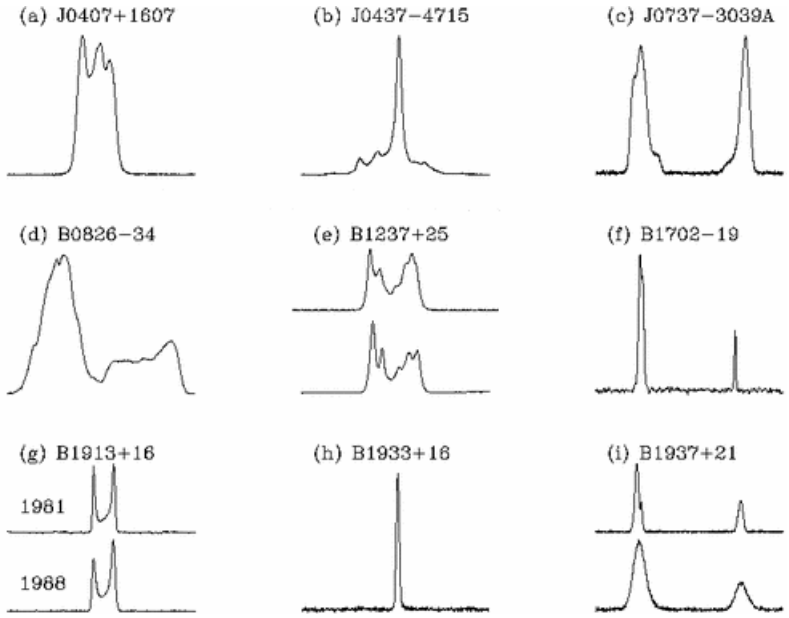

Pulsar in Crab Nebula: with a secondary pulse at $\frac{1}{2}$ period

Period (duty cycle)

Mainly in radio (Crab pulsar in optical band, X and gamma)

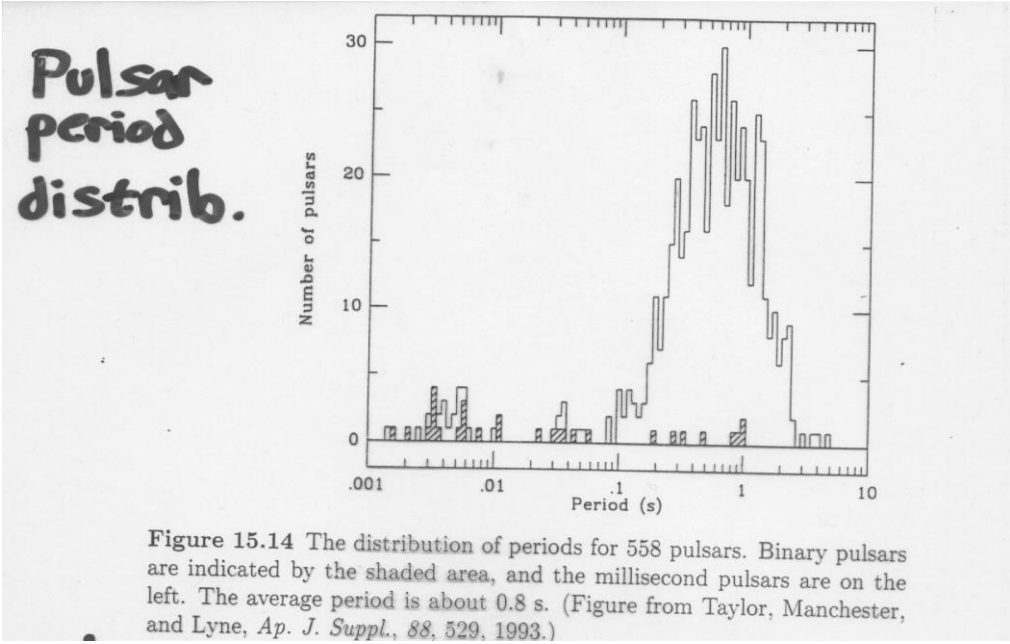

Figure 15.14 The distribution of periods for 558 pulsars. Binary pulsars are indicated by the shaded area, and the millisecond pulsars are on the left. The average period is about 0.8 s. (Figure from Taylor, Manchester, and Lyne, *Ap. J. Suppl.*, *88*, 529, 1993.)

Average value ~0.8 s

Tail: millisec pulsars

Pulsar Timing Irregularities

Most pulsars are observed to have remarkable rotational stability, mainly due to their isolated environments and large, stable moments of inertia. Therefore, the detection of timing irregularities in their pulsed emission requires dedicated observation of many pulsars to increase the possibility that irregular rotational behaviour is found.

Glitches, micro pulses
+ slow variations, on timescale of min or hours, correlated in the 0.1-10 MHz band, due to interstellar scintillation.

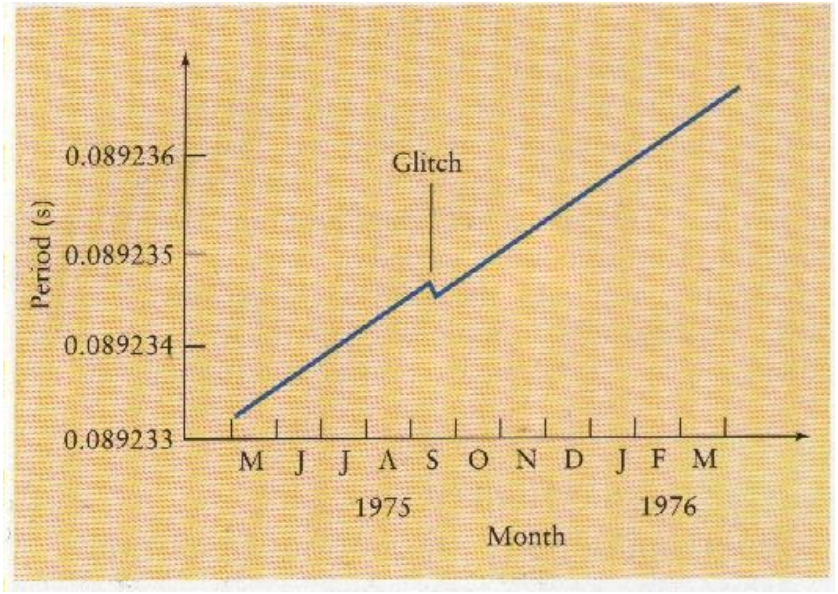

Glitches are discontinuous changes in the rotation period, accompanied by quasi-exponential recoveries with timescales of hours up to years. Such variation can be interpreted as changes in the pulsar environment and/or neutron star interior.

Pulsar Timing Irregularities

Most pulsars are observed to have remarkable rotational stability, mainly due to their isolated environments and large, stable moments of inertia. Therefore, the detection of timing irregularities in their pulsed emission requires dedicated observation of many pulsars to increase the possibility that irregular rotational behaviour is found.

There are two types of timing irregularities in pulsar timing: "timing-noise" which is characterised by a random phase wandering in pulses relative to the general slow-down model, and "glitches" which are discontinuous changes in the rotation period, accompanied by quasi-exponential recoveries with timescales of hours up to years. Such variation can be interpreted as changes in the pulsar environment and/or neutron star interior. This irregular behaviour is not isolated to changes in rotational frequency and pulse phase, but also extends to the intensity and timescale of observed emission, as well as variation in the shapes of pulse profiles.

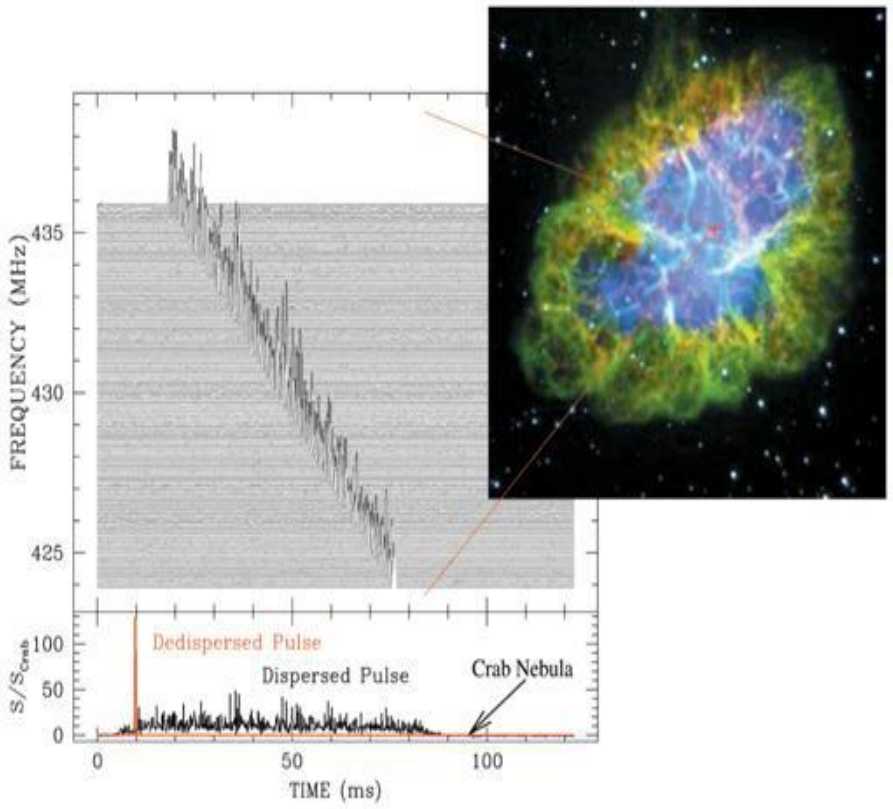

The de-dispersed pulses show micro-pulses

Pulsar Timing Irregularities

Individual pulses resolved into **micro pulses**

- Generally at low frequencies
- Though correlated of wide frequency range
- Often Quasi-periodic - frequency independent

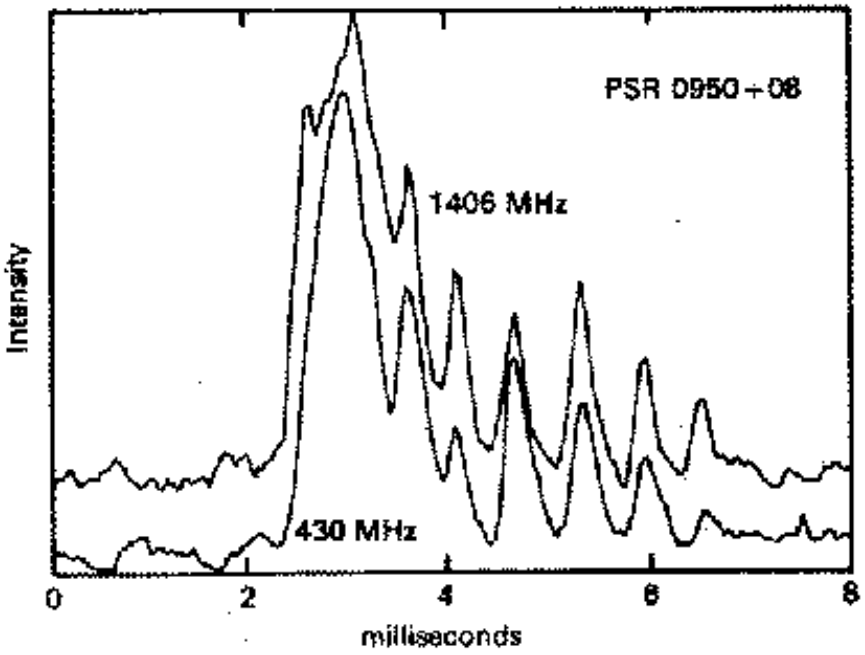

The emitted pulse , with all its frequencies peaking at the same time, is gradually dispersed as it travels to Earth; the lower frequencies are slower than the higher ones, and the delay depends on the DM:

$$\Delta t \cong 4.15\times10^{3}\left(\frac{1}{\nu_1^2}-\frac{1}{\nu_2^2}\right)DM$$

Measuring Δt at two frequencies → DM →assuming a distribution for n_e (ISM free e density) the pulsar distance can be derived by:

$$DM = \int_0^d n_e dl$$

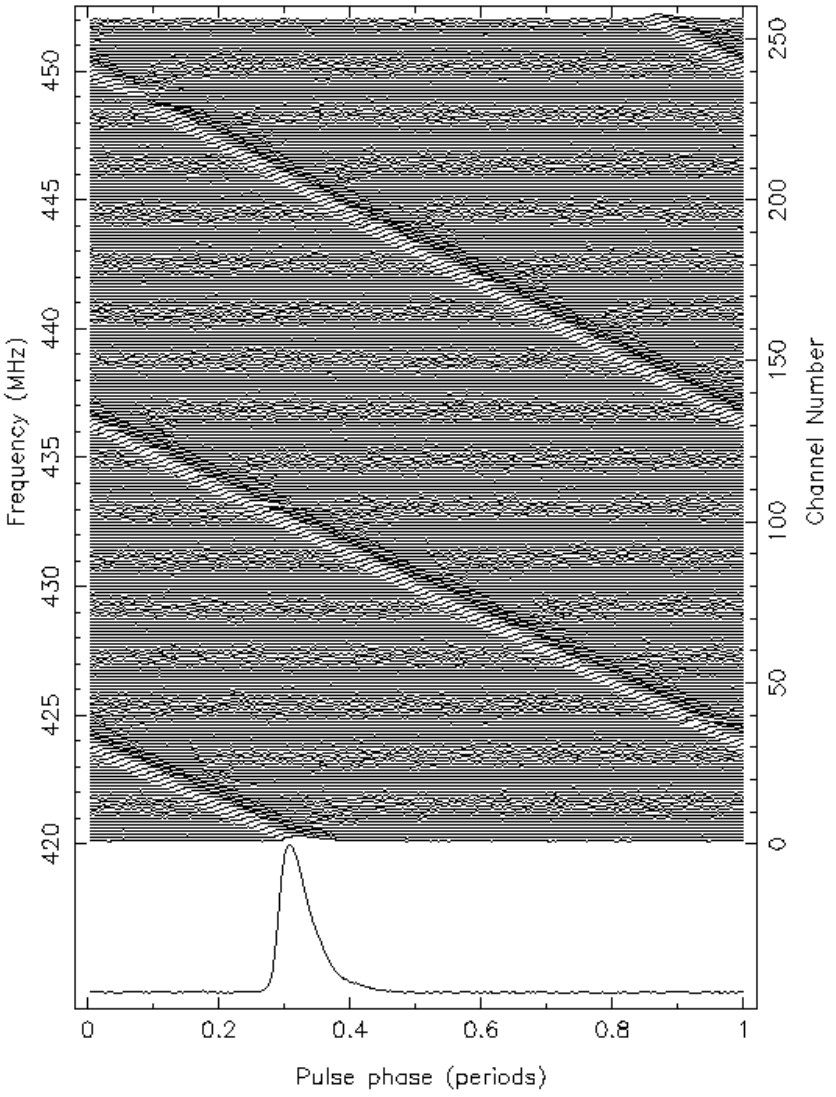

Dispersion of a signal due to the ISM; the recovered signal is shown in the bottom

Radio spectra

Taking median spectra, due to variability of pulse amplitude,

$$S \propto \nu^{\alpha}; \alpha \sim -1/-3$$

$$\langle \alpha \rangle \sim -1.5$$

- Peak between 100 and 500 MHz
(probably not due to free-free absorption, the exponential behaviour is not correct, but intrisic of the emission mechanism)
- Steepening at frequency > 1 GHz

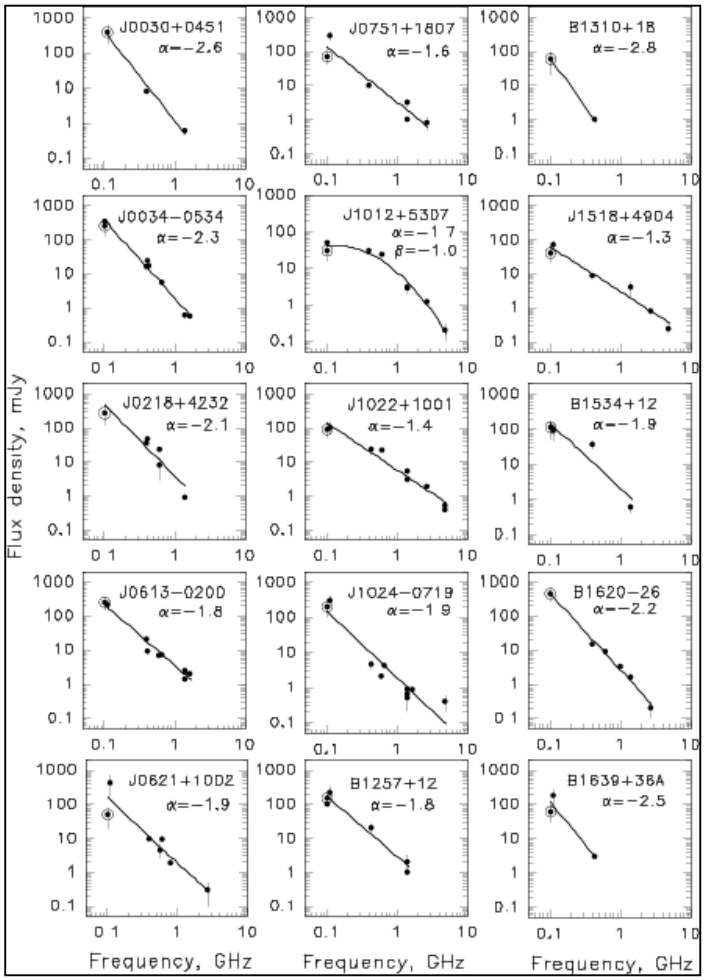

In the Crab Nebula probably two mechanism to product radio and high energy pulses.

Polarization and luminosity

- High % of linear polarization > circular polarization (~20%)
- Polarization angle: regular change inside the pulse and from pulse to pulse

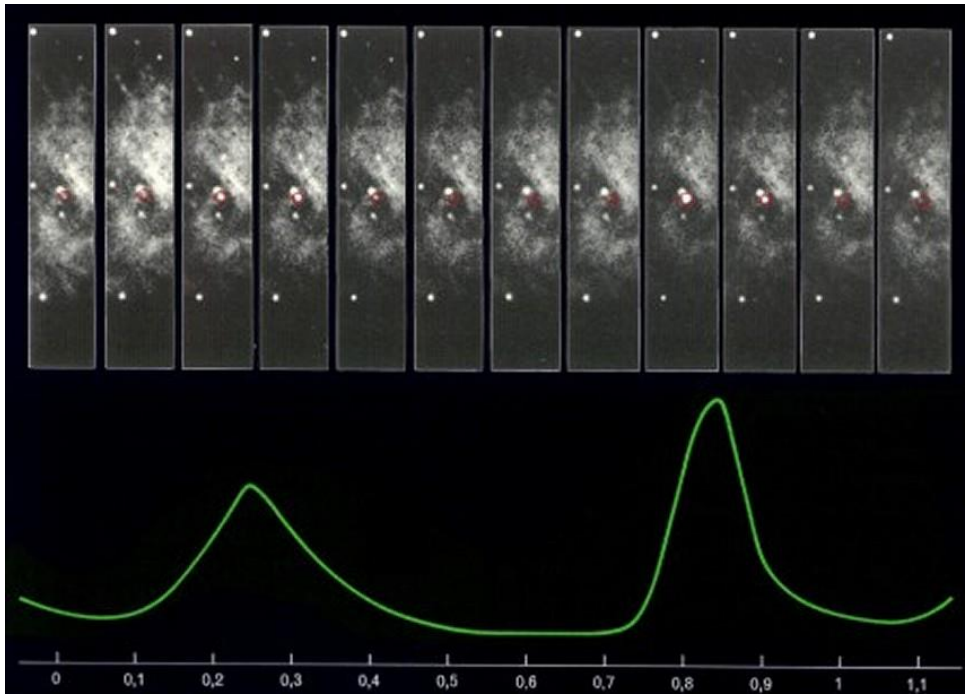

Crab pulsar (red circle): period 33ms at optical wavelength

Luminosity: 10^{20} – 10^{24} W in radio domain

Vela pulsar ~10^{29} W in gamma ray

Crab nebula pulsar ~10^{29}W in X-ray and ~10^{30}W in gamma ray

Periods

High stability: $1/10^{10}$

Periods: from 1.5 ms to 8.5s

Slow sistematic variations:

10^{-13}s/day (Crab 3.5×10^{-8} s/day)

Distribution of radio pulsars, radio-quiet pulsars, soft-gamma repeaters and anomalous X-ray pulsars (AXPs) in the P-dP/dt plane. Binary systems by a circle.

$\dot{P}$

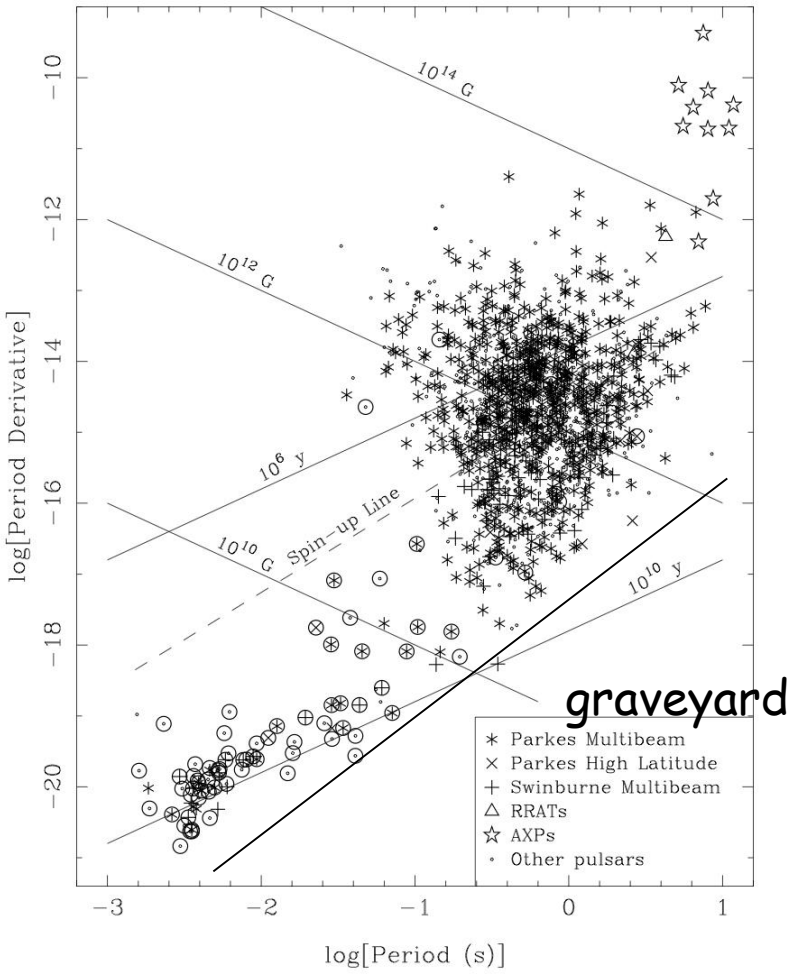

P

Lines of constant pulsar characteristic age and surface dipole magnetic field strength

$$\tau_c = \frac{P}{2\dot{P}} \qquad B_s \propto (P\dot{P})^{1/2}$$

Graveyard=no radio pulsars predicted by theoretical models

30 msec pulsars in Terzan 5 (Ransom+2005, Hessel+2006)

Periods

Name	P (sec)	(# turns in 1 sec)
PSR B0329+54	P=0.714519	1.4
PSR B0833-45=The Vela Pulsar	P=0.089	11
PSR B0531+21=The Crab Pulsar	P=0.033	30
PSR J0437-4715	P=0.0057	174
PSR B1937+21	P=0.00155780644887275	642
PSR J1748-2446	P=0.0013966	716

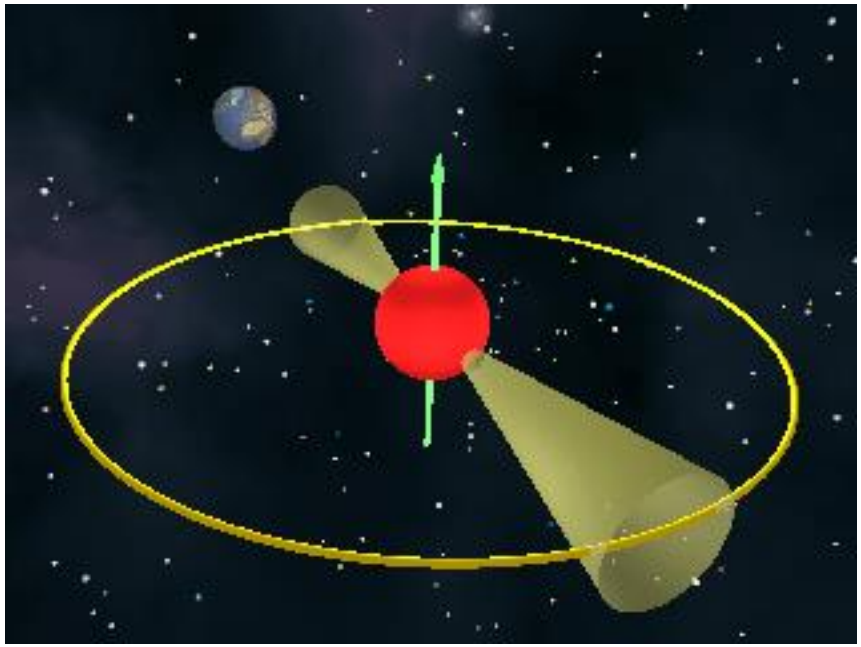

Using observations on timescale of years the fundamental quantities can be determined with these errors

- Period $\pm 10^{-12}\, s$
- Derivative $\pm 10^{-18}$
- Coordinates $0.1 arc\sec$

Proper motions

OB associations in the solar neighborhood projected onto the Galactic plane (de Zeeuw+ 1999). **The diamonds mark the current positions of two pulsars** (B1929, B2021), and their motion was traced backwards in time for each pulsar's spin-down age. The different colored points represent possible birthplaces computed in a Monte-Carlo fashion:

Dark blue:from uncertainty in the proper motion only

Cyan: from uncertainty in the parallax only

Green: from the unmeasured radial velocity

Magenta: all three sources of uncertainty taken simultaneously

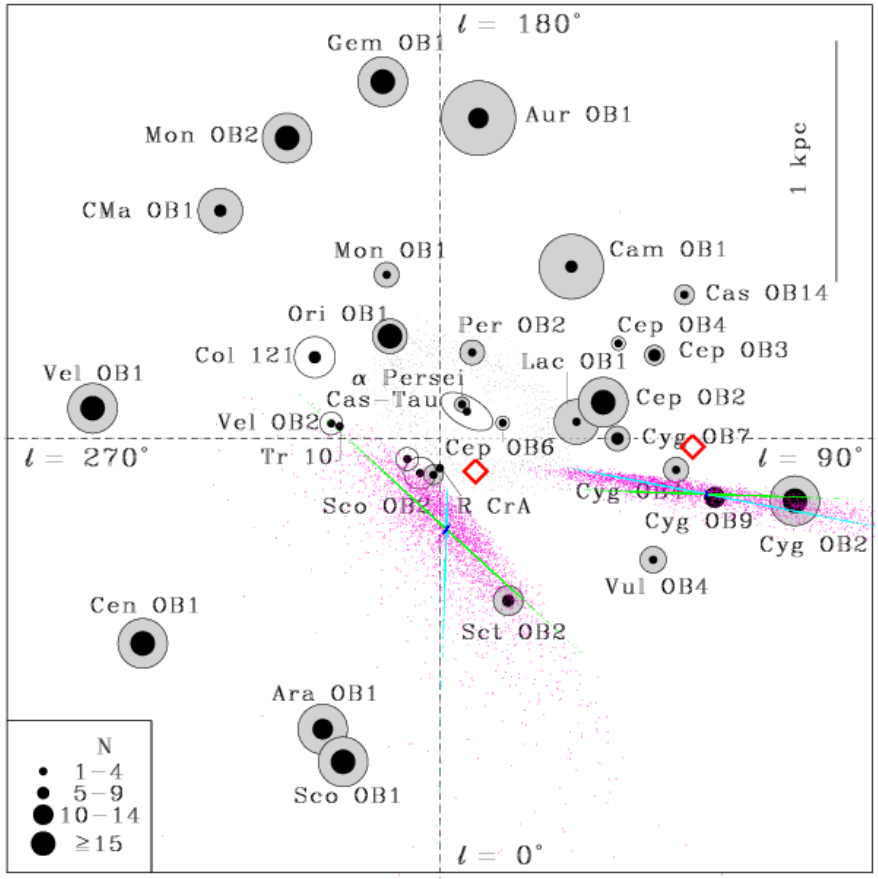

Knowing the distance of the pulsar the trasverse velocity is obtained: mean value 200 km/s (> tipycal velocity of the stars in the disc)

Distances

- From the distance of the SNR (few cases)
- From HI observations
- From DM using a mean electronic density

(n_e ~0.03 cm^{-3} uncertainty introduces a factor 2 in the value of distance)

$$DM = \int_0^L n_e dl$$

Height above the galactic plane (z)

Pulsars are concentrated in the galactic plane

$$N_P(|z|) = N_0 e^{-|z|/h_P} \qquad h_P = (230 \pm 20)\,pc$$

The charactestic scale h_P is

>> the distribution of OB stars (~80pc) and of SNR (<100 pc), but the pulsars have high velocity (up to 500 km/s)

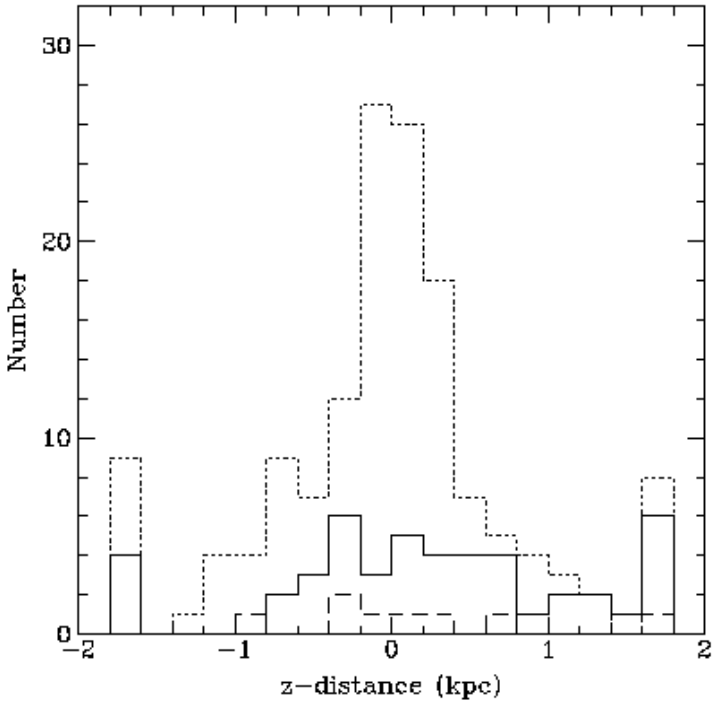

The observed distribution of pulsar distances above the galactic plane. Dotted curve is the total known population, solid curve is the Parkes survey.

Radial distribution

Selection effect due to the faint pulsars

Yusifov & Küçük, 2004

Decrease for R>6-7 kpc

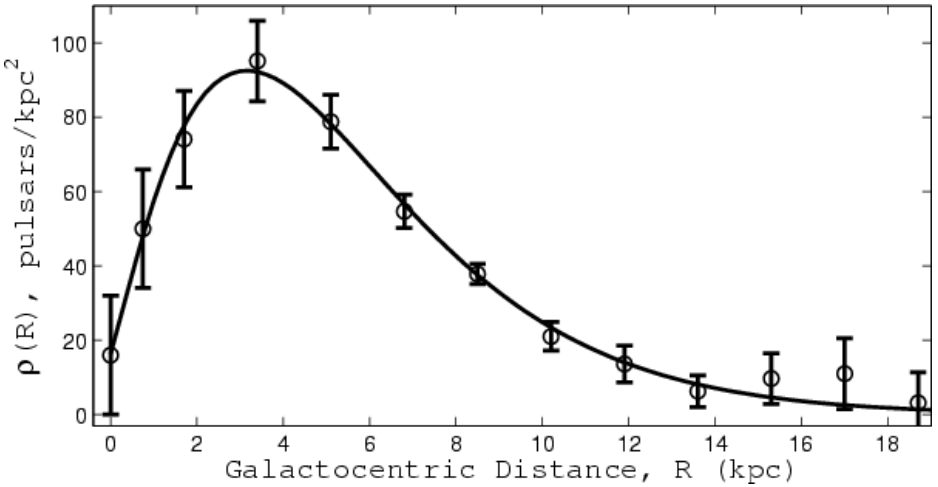

The maximum galactocentric distribution of pulsars is located at 3.2 +/-0.4 kpc.

The surface density of pulsars near the Galactic center is equal to or slightly higher than that in the solar neighborhood.

Pulsars known

about 2300

If we consider the spatial distribution (distance) of the known pulsars we get an estimate of the total number ~ 150 thousands in our galaxy.
Recent result (Yusifov & Küçük, 2004) potentially observable pulsars in the Galaxy: $(24+/-3)x10^3$ and $(240+/-30)x10^3$ before and after applying beaming correction according the Tauris & Manchester (1998) beaming model.

If we attribute an average age of 5 million years we infer the formation of a pulsar every 30-120 yr

consistent with the formation rate of SNR

However, we must correct the number for:
- more distant and weak sources may be under-represented
- pulsars are revealed if the beam is at a small angle to the LOS
- the magnetic field decays with age, then old pulsars are underepresented

SKA

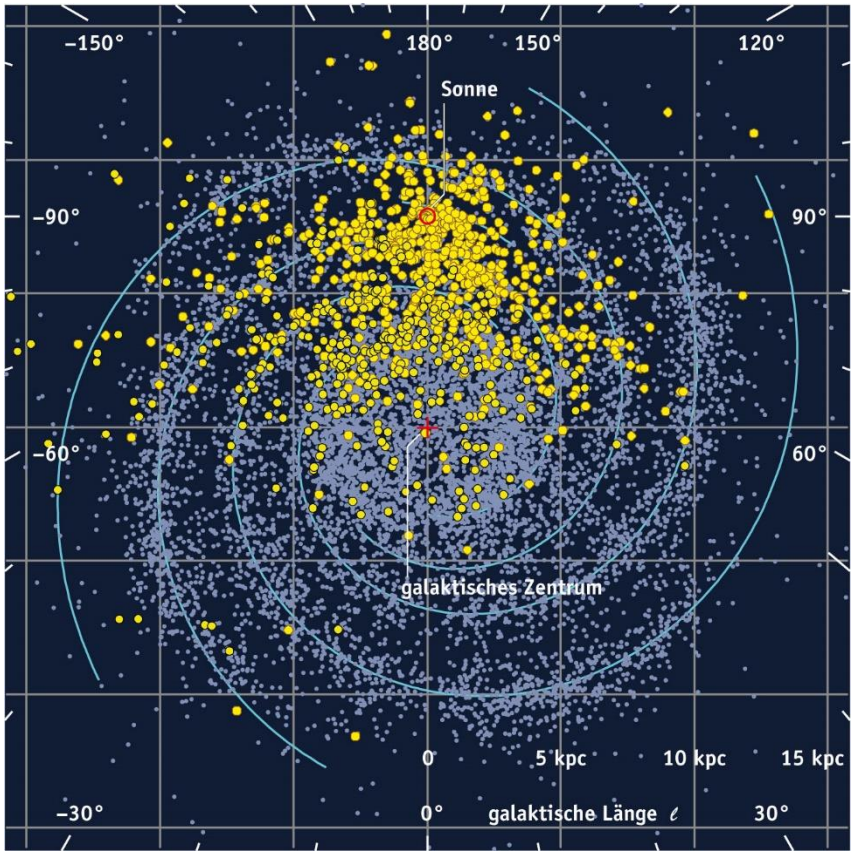

yellow=known, grey= SKA pulsars

Luminosity function

Knowing the distance → LF, the number of pulsars per volume unit with the luminosity > L

LF

- is prop. to L^{-1} over 4 orders of magnitude
- is flatter for L< 3mJy kpc^2

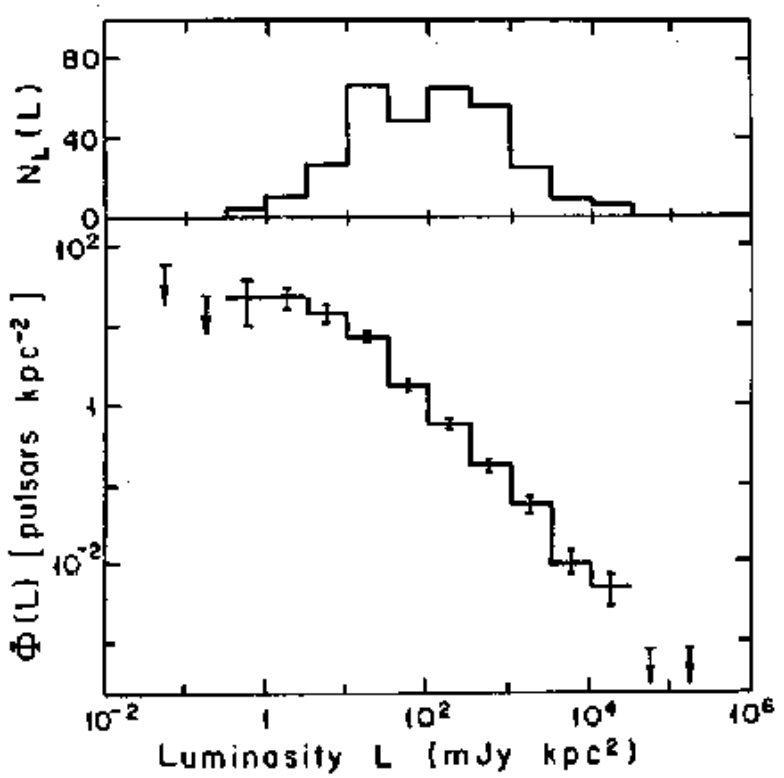

Neutron stars

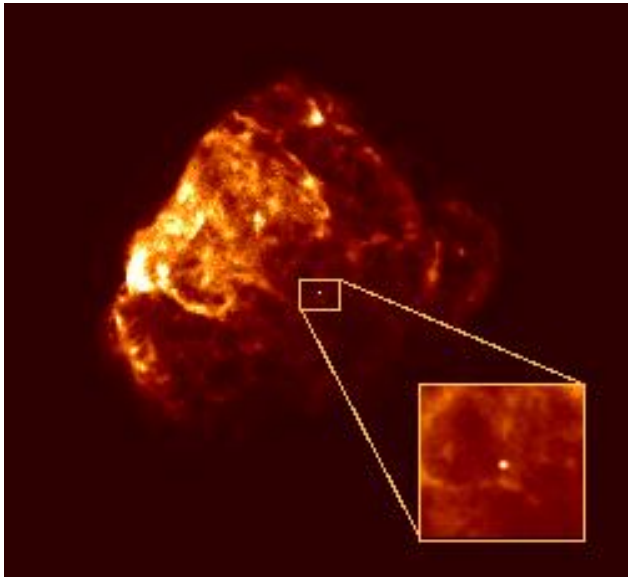

Neutron stars: compact objects created in the cores of massive stars during SN explosions or in x-ray binaries with a normal star.

The core collapses and crushes together every proton with a corresponding electron turning each electron-proton pair into a neutron.
The neutrons can often stop the collapse and remain as a neutron star.

Neutron stars can be observed occasionally:
Puppis A –in x-ray, above – an extremely small and hot star within a SNR.
They are seen when they are a pulsar or part of an X-ray binary.

The history of Neutron Stars

Chandrasekhar (1931) WDs collapse at > 1.44 Msun

Baade & Zwicky (1934) proposed: existence of neutron stars
their formation in supernovae
radius of approximately 10 km

Oppenheimer & Volkoff (1939)
Evaluated first equation of state (i.e. relation between density and pressure)
Mass > 1.4 Msun
Radius ~ 10 km
Density > 10^{14}g cm $^{-3}$

Pacini (1967) proposed:
electromagnetic waves from rotating neutron stars
such a star may power the Crab nebula
i.e. **PULSARS**

Mass measurements

Measurements from timing observations of binary pulsars

consistent with a typical pulsar

$$Mass \geq 1.4 M_{sun}$$

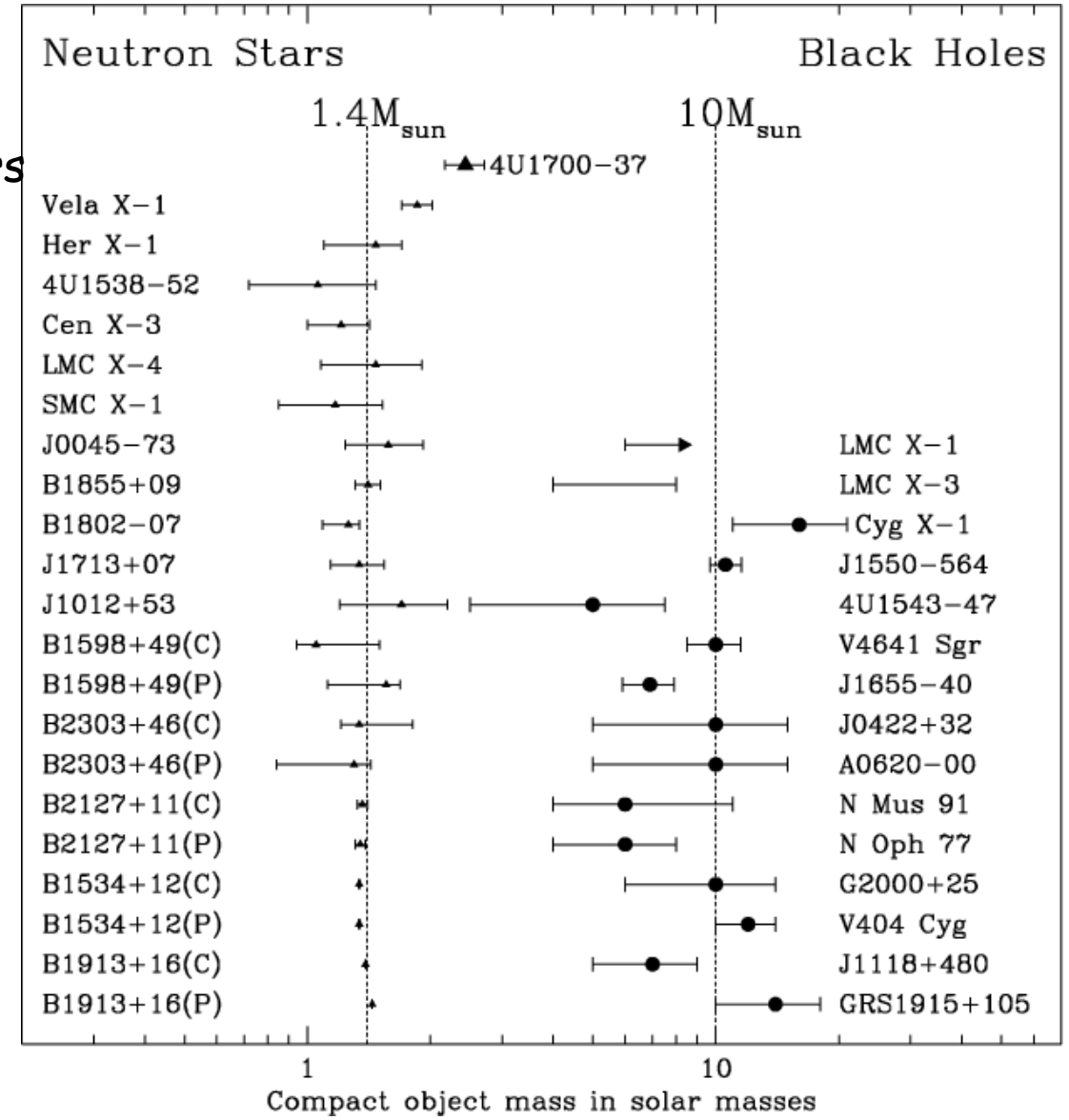

Radius determination

Difficult to obtain, methods:

- thermal emission from neutron star surface at optical and X-ray frequencies, where the observed luminosity can be used to infer the size of emitting region. Strong gravitational fields and atmospheres of NS complicate calculations.
- Based on arguments that the speed of sound should be smaller than the speed of light in a NS and that the equation of state provides a smooth transition from low to high densities
- NS must be stable against break-up due to centrifugal forces

Most models predict a radius ~10-12 km (only 3 times larger than the Schwarzschild radius→almost BH)

Moment of Inertia

Moment of inertia is $I = kMR^2$ where k=2/5=0.4 for a sphere of uniform density.

For a NS k depends on the equation of state. Most models predict k=0.30-0.45 for a mass/radius range 0.10-0.20 Msol/km

The adopted value for M=1.4Msol, R=10km and k=0.4 is:

$I=10^{45}$ g cm^2

Structure (most NS models)

Using the previous values the average mass density is

$$\langle \rho \rangle = 6.7 \cdot 10^{17}\, kgm^{-3}$$

NS is not a uniform sphere→ observations of glitches indicate a solid crust that is tied to a liquid interior.

Solid crust of iron nuclei and a sea of degenerate electrons
Largest fraction of NS is a sea of free, superfluid neutrons + ~5% of electrons and protons

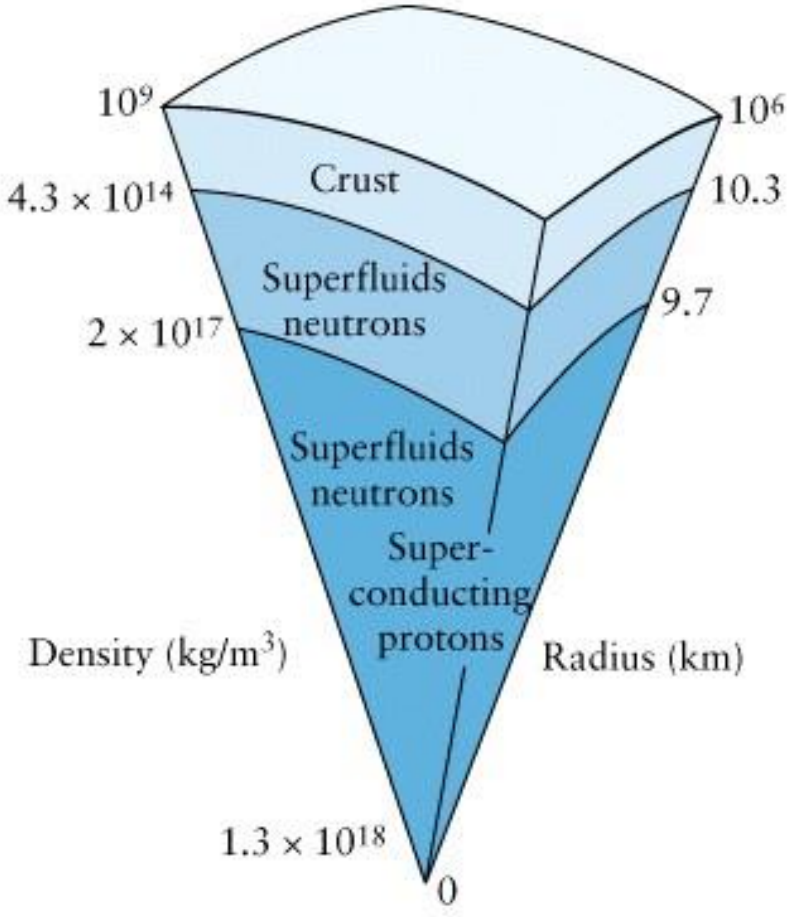

Spin evolution

Pulse periods are observed to increase with time. The loss of rotational kinetic energy (spin-down luminosity, i.e. the total power output by the NS) is:

$$\dot{E} \equiv -\frac{dE_{rot}}{dt} = -\frac{d(I\omega^2/2)}{dt} = -I\omega\dot{\omega} = 4\pi I P^{-3}\dot{P} \qquad \omega = \frac{2\pi}{P}$$

$$\dot{E} \cong 3.95 \cdot 10^{31} erg/s \left(\frac{\dot{P}}{10^{-15}}\right)\left(\frac{P}{s}\right)^{-3}$$

The bulk of the rotation energy is converted into high-energy radiation and, in particular, in magnetic dipole radiation and pulsar wind. Only a small fraction is converted into radio emssion.

Braking index

Pulsars have strong dipole magnetic fields. According to classical elettrodynamics (Jackson, 1962) a rotating magnetic dipole with moment **m** radiated an electromagnetic wave at its rotation frequency. The radiation power

$$\dot{E}_{dipole} = \frac{2}{3c^3}\left|\vec{m}\right|^2 \omega^4 \sin^2\alpha \qquad (1)$$

α angle between the rotation axis and the magnetic dipole moment

By equating with the spin-down luminosity with (1):

$$\dot{\omega} = -\left(\frac{2\left|\vec{m}\right|^2 \sin^2\alpha}{3Ic^3}\right)\omega^3$$

Espressing as a power law and in term of frequency

$$\dot{\nu} = -K\nu^n$$

n is the braking index

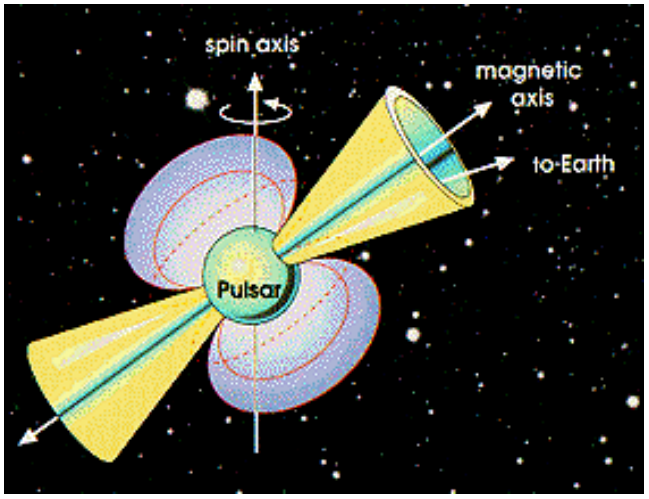

Braking index

For pure magnetic dipole braking n=3, other dissipation mechanisms may exist (e.g. wind of outflowing particles) that also carry away some of the rotational kinetic energy.

The braking index can be determined if the second derivative can be measured. Differentiating and eliminating K:

$$\dot{\nu} = -K\nu^n \longrightarrow n = \frac{\nu\ddot{\nu}}{\dot{\nu}^2}$$

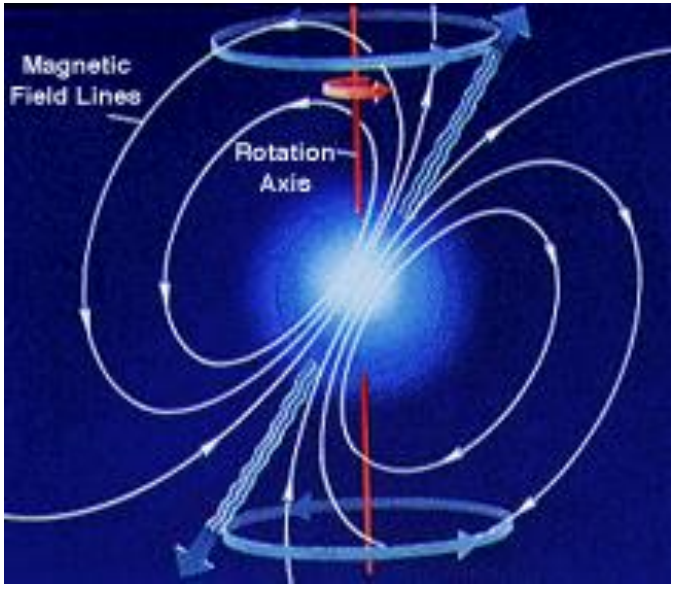

For a few pulsars the second derivative can be maesured and n is in the range 1.4-2.9.

n=3 is not completely correct

Age estimates

$\dot{\nu} = -K\nu^n$ Espress the equation in term of the period:

$$\dot{P} = KP^{2-n}$$

The eq. can be integrated, assuming K constant ed n not equal to 1:

$$T = \frac{P}{(n-1)\dot{P}}\left[1-\left(\frac{P_0}{P}\right)^{n-1}\right]$$

Considering the spin period at birth much shorter than the present value and n=3, the characteristic age is:

$$P_0 << P$$

$$\tau_c \equiv \frac{P}{2\dot{P}} \cong 15.8 Myr \left(\frac{P}{s}\right)\left(\frac{\dot{P}}{10^{-15}}\right)^{-1}$$

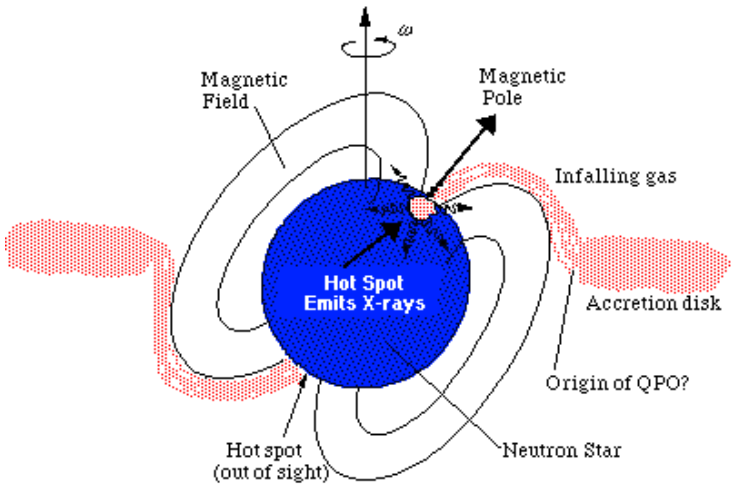

Age estimates

The characteristic ages are in agreement with the known ages of Crab and Vela pulsars

Discrepancies with known ages are for example for the young pulsar J0205+6449, born in a SN (AD 1181)

Kinematic age: from the distribution in z above the galactic plane, considering that the pulsars were born at z=0 with a velocity distribution similar to the observed one.

Agreement between the characteristic and kinematic ages for ages less than 10^7 yr. Possible solutions for the old pulsars: dP/dt decreases with time or height above the galactic plane is the maximum and they are falling back.

Birth period

Using the eq. and the characteristic age:

$$T = \frac{P}{(n-1)\dot{P}}\left[1-\left(\frac{P_0}{P}\right)^{n-1}\right]$$

$$P_0 = P\left[1-\frac{(n-1)}{2}\frac{T}{\tau_c}\right]$$

If the true age of the pulsar is known (e.g. associated with an historical SNR) and n has been measured, the birth period can be estimated.

Recent estimates suggest a wide range of initial spin periods from 14 to 140 ms.

Magnetic field strength

Values have been obtained for X-ray binaries and from an isolated pulsar, in the range 10^{11}-10^{12} G.

An estimated can be obtained by assuming that the spin-down process is dominated by dipole braking. The relation between magnetic dipole and B is:

$$B \approx \left|\vec{m}\right| / r^3$$

Rearranging this eq.

$$\dot{\omega} = -\left(\frac{2\left|\vec{m}\right|^2 \sin^2 \alpha}{3Ic^3} \right) \omega^3$$

B at the surface is:

$$B_S \equiv B(r = R) = \sqrt{\frac{3c^3}{8\pi} \frac{I}{R^6 \sin^2 \alpha} P\dot{P}}$$

Assuming the canonical value for I and R and alpha=90deg.

$$B_s(G) = 3.2 \cdot 10^{19} \sqrt{P\dot{P}} \cong 10^{12} \left(\frac{\dot{P}}{10^{-15}} \right)^{1/2} \left(\frac{P}{s} \right)^{1/2}$$

Characteristic magnetic field is essentially an order of magnitude estimate.

Pulsar: highly magnetised, rotating super conducting sphere, leading to external electric field and to the extraction of plasma from the NS surface.
This plasma is the pulsar magnetosphere.
The model of G&J does not describe a realistic case, but it illustrates some basic principles.

At any point r inside the sphere a force-free state is obtained:

$$\vec{E} + \frac{1}{c}(\vec{\omega} \times \vec{r}) \times \vec{B} = 0$$

If vacuum is outside the surface charges induce an external quadrupole field, in polar coordinates:

$$\Phi(r, \vartheta) = \frac{B_S \omega R^5}{6cr^3}(3\cos^2 \vartheta - 1)$$

The corresponding electric field at the surface is:

$$E_{\square} = \left(\frac{\vec{E} \cdot \vec{B}}{B} \right)_{r=R} = -\frac{\omega B_S R}{c} \cos^3 \vartheta$$

It causes an electrical force on the charged particles that exceeds gravity by 10 or more orders of magnitude.

The charge distribution of the dense surrounding medium is:

$$\rho_e(r,\vartheta) = \frac{1}{4\pi}\nabla\cdot\vec{E} = -\frac{\omega B}{2\pi c} = -\frac{B_S \omega R^2}{4\pi c r^3}(3\cos^3\vartheta - 1)$$

Charges above the equatorial region will be of opposite sign to charges above magnetic poles, the density changes sign for $\cos\vartheta = \sqrt{1/3}$

Assuming complete charge separation, the number density at the magnetic pole $(r = R, \vartheta = 0)$

$$n = \frac{\rho_e}{e} = \frac{\omega B_S}{2\pi c e} = \frac{B_S}{ceP} = 7\cdot 10^{10}\, cm^{-3}\left(\frac{P}{s}\right)^{-1/2}\left(\frac{\dot{P}}{10^{-15}}\right)^{-1/2}$$

is the Goldreich-Julian density, represents a maximum value unless further process exist

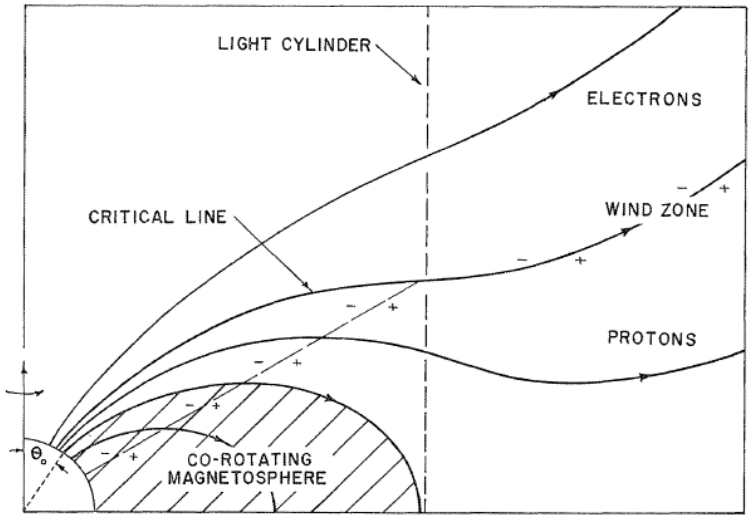

The plasma outside the NS experiences the same **E-B** field as the NS interior, forcing it to co-rotate rigidly with the star. The co-rotation can only be maintained up to a maximum distance where the velocity of plasma reaches c.

This limit defines a surface known as light cylinder with radius:

$$R_{LC} = \frac{c}{\omega} = \frac{cP}{2\pi} \cong 4.77 \cdot 10^4 km \left(\frac{P}{s} \right)$$

The magnetic field at the light cylinder radius is:

$$B_{LC} = B_S \left(\frac{\omega R}{c} \right)^3 \cong 9.2 \left(\frac{P}{s} \right)^{-5/2} \left(\frac{\dot{P}}{10^{-15}} \right)^{1/2} G$$

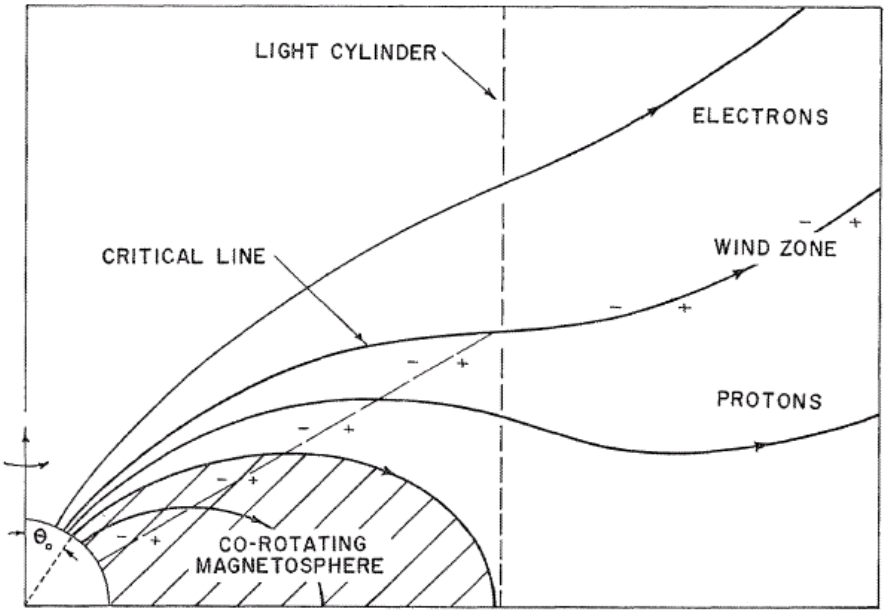

Toy model for the rotating neutron star and its magnetosphere

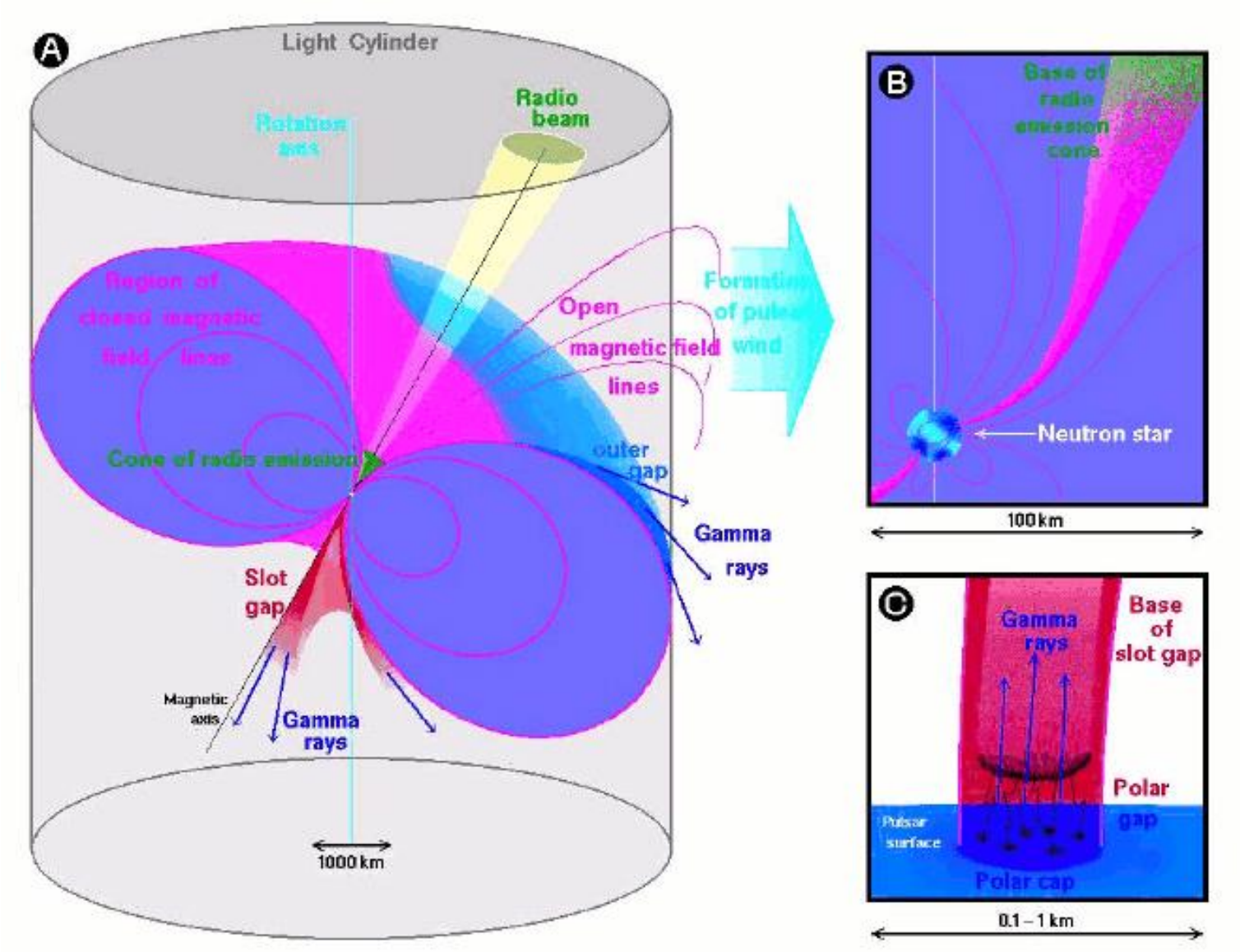

Energetics

(see Lorimer & Kramer " Handbook of pulsar astronomy" for details)

A correct estimate of the Luminosity is difficult:
a) The radio emission is highly beamed
b) We observe only one-dimensional cut of an emission beam of unknown shape
c) The flux density spectrum does not have the same shape for all the pulsars
d) Reliable estimates of pulsars distances are difficult to obtain
e) Pulsar flux densities may be affected by scintillation
Assuming that cut observed is representative of the whole beam:

$$L = \Omega d^2 \int S(f)_{peak}\, df$$

d=distance of the pulsar

Omega=solid angle of the pulsar beam

$$L = 7.4 \cdot 10^{27} \left(\frac{d}{kpc} \right)^2 \left(\frac{S_{1400}}{mJy} \right) erg/s$$

Brightness Temperature

$$T_B = \frac{S_{peak}}{2\pi k}\left(\frac{f\Delta t}{d}\right)^2 \cong 10^{30}\,\frac{S_{peak}}{Jy}\left(\frac{f}{GHz}\right)^{-2}\left(\frac{\Delta t}{\mu s}\right)^{-2}\left(\frac{d}{kpc}\right)^2 K$$

Inserting the value for the Crab pulsar the brightness temperature exceeds 10^{35} K ruled out all incoherent mechanisms

Optical and X-ray emission: $T_B \sim 10^{10} - 10^6$ K (Vela and Crab pulsars) compatible with incoherent emission

Two different processes for radio and optical-X-gamma emissions

Radio Emission

Any proposed radiation process has not only to explain the coherency and high degree of polarization of the emission, but also has to work efficiently over nearly 4 orders of magnitude in rotation period and 6 order of magnitude in magnetic field.

Similarly, pulsar emission is observed from about 100 MHz to 100 GHz, requiring a very broad-band emission process.

More than 40 years after the discovery of pulsars, and despite many attempts to assemble and analyse the very detailed observational data, it is still not possible to give a clear exposition of the processes by which pulsars emit beams of radio waves.

In both radio and gamma emissions, the source of energy is the enormous electric field which is induced by the rapid rotation of the highly magnetised NS.

The radio emission is coherent emission from a plasma created by the primary particle stream.

Solar system tests provide a number of very stringent tests in General Relativity, however to test strong-field predictions binary pulsars are and will remain the only way.
9 double neutron star binaries (DNS) are known with orbital periods from 2.4 h to 18.8 days.

Double systems with both "compact" stars (NS-NS) no mass transfer, no tidal effects, they can be treated as a simple pair of point masses.

e.g. PSR B1913+16
1993: Nobel Prize in Physics:
Russell Hulse & Joseph Taylor
(Princeton University)
discovery of a pulsar (in 1974)
in a binary system, in orbit with another star around a common centre of mass.

orbital shrinkage ~ 1cm/day → orbital decay with release of gravitational waves

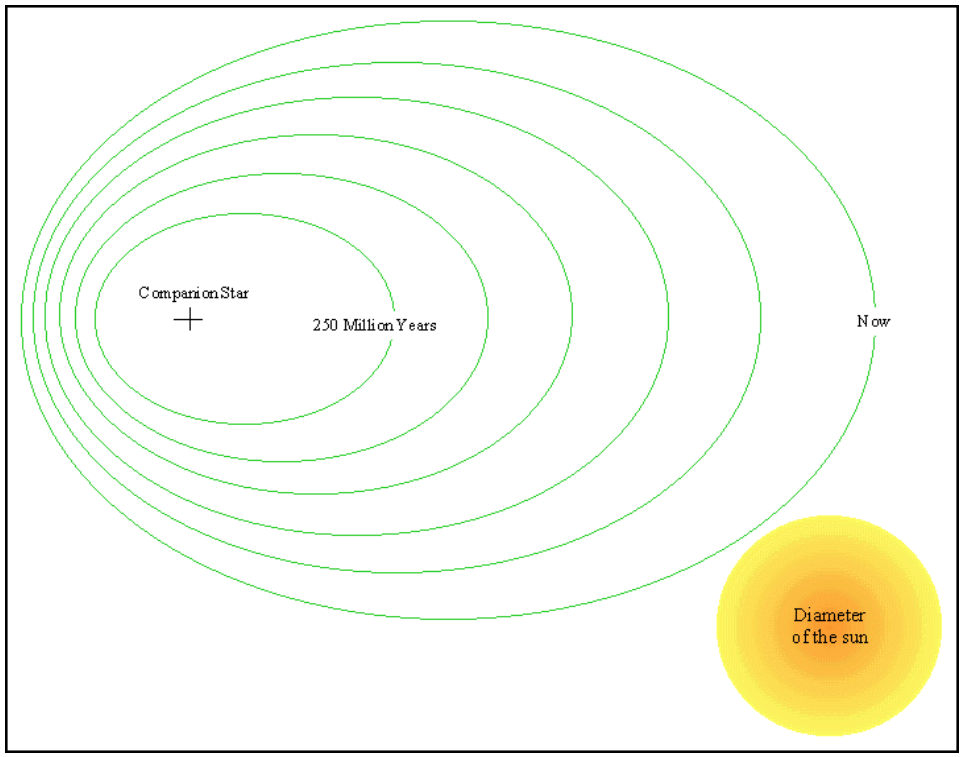

Pulsars

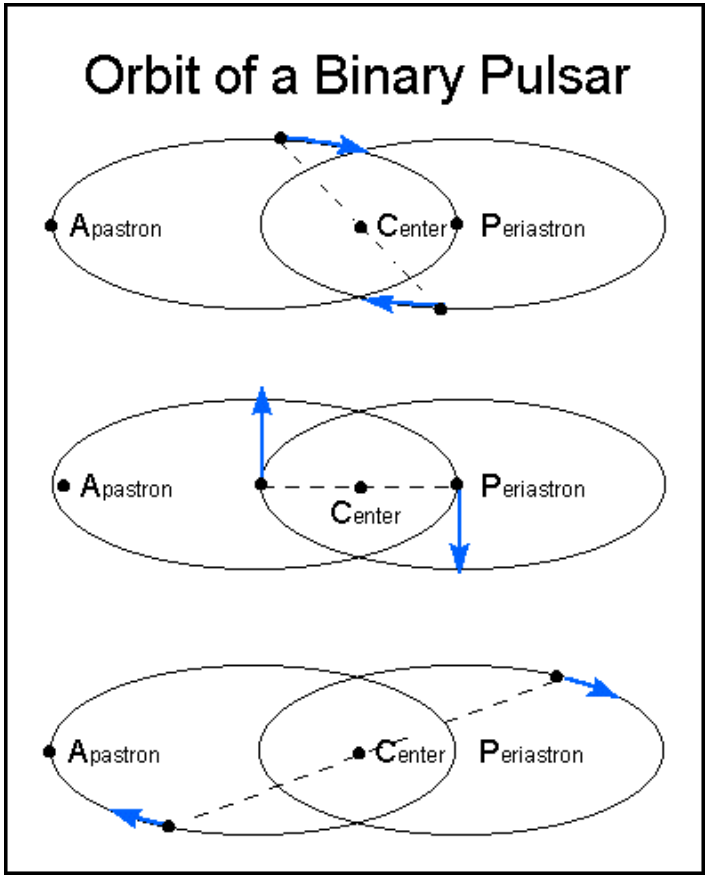
Orbit of a Binary Pulsar
Apastron
Center
Periastron
Apastron
Center
Periastron
Apastron
Center
Periastron

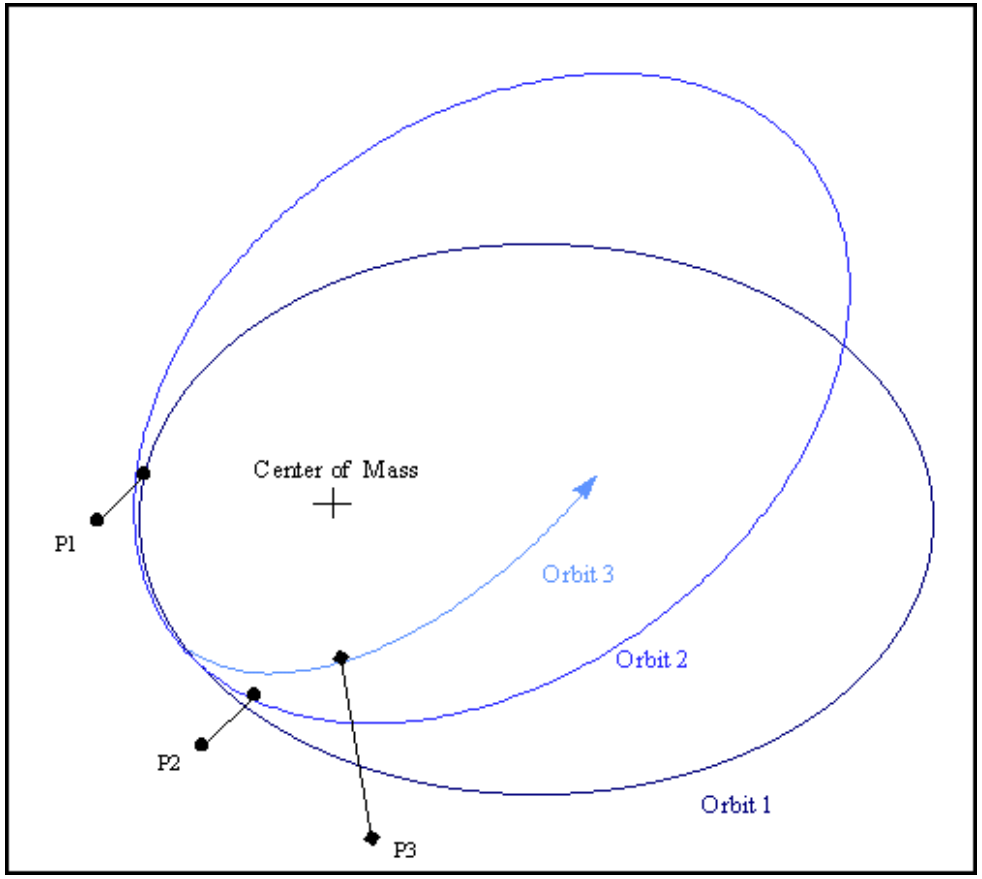
Center of Mass
P1
Orbit 3
Orbit 2
P2
Orbit 1
P3

Binary system

PSR B1913+16: shift of the periastron passage as a function of time.

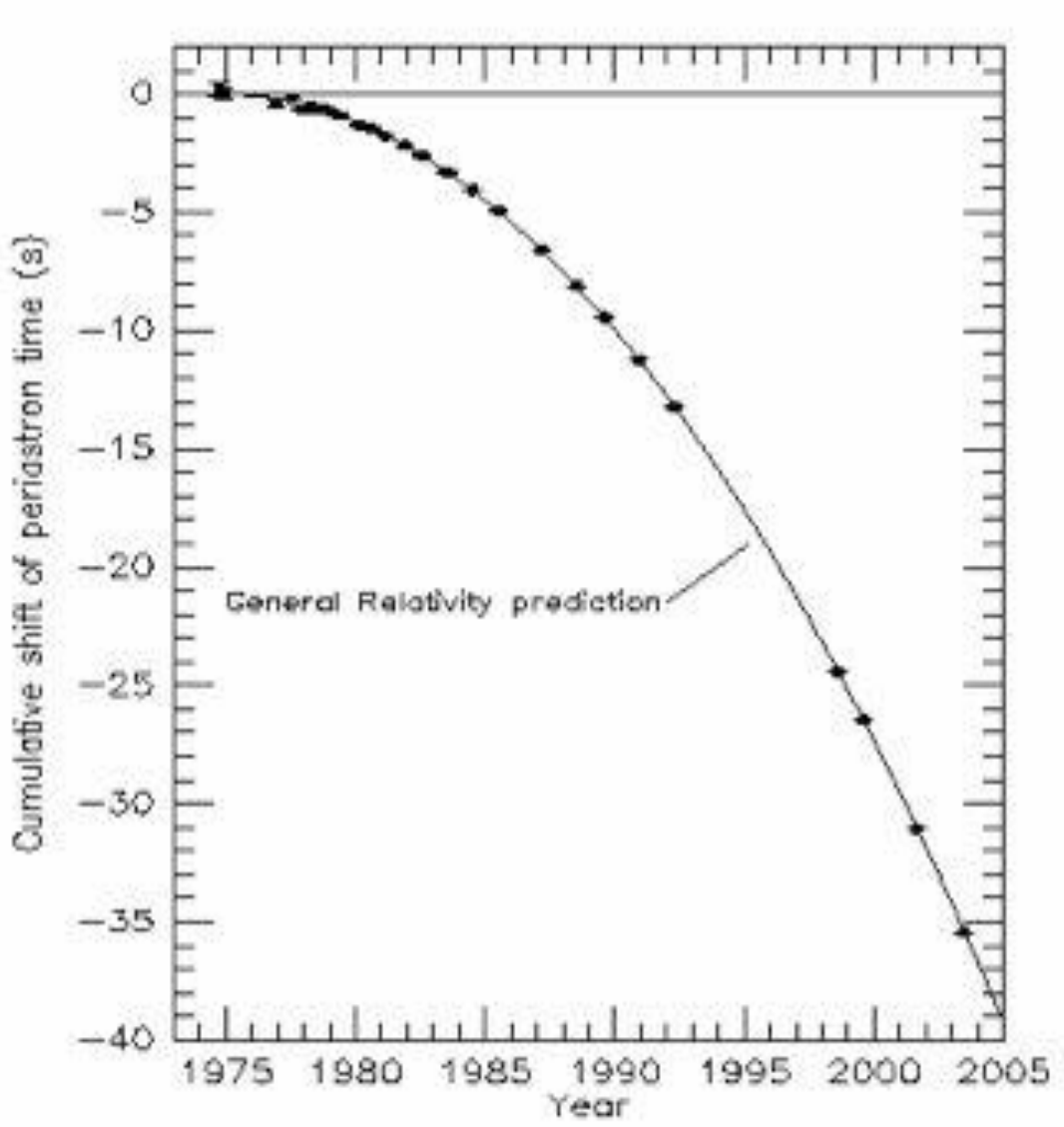

Keplerian Parameters

Kepler's laws can be used to describe a binary system in terms of five parameters:

- Orbital period, P_b
- Projected semi-major orbital axis, $a_p \sin i$
- Orbital eccentricity, e
- Longitude of periastron, ω
- Epoch of periastron passage, T_0

Tests of GR are possible by the measurements of the "post-Keplerian" (PK) parameters, relativistic additions to the standard Keplerian orbit parameters.

Relativistic effects due to strong gravitational fields and high orbital velocities produce observable signature in the time residuals.

Periastron precession

$$\dot{\omega} = 3\left(\frac{P_b}{2\pi}\right)^{-5/3}(T_\odot M)^{2/3}(1-e^2)^{-1}$$

Gravitational redshift

$$\gamma = e\left(\frac{P_b}{2\pi}\right)^{1/3} T_\odot^{2/3} M^{-4/3} m_2 (m_1 + 2m_2)$$

Orbital decay

$$\dot{P}_b = -\frac{192\pi}{5}\left(\frac{P_b}{2\pi}\right)^{-5/3}\left(1+\frac{73}{24}e^2+\frac{37}{96}e^4\right)(1-e^2)^{-7/2} T_\odot^{5/3} m_1 m_2 M^{-1/3}$$

Range of Shapiro Delay

$$r = T_\odot m_2$$

Shape of Shapiro Delay

$$s = x\left(\frac{P_b}{2\pi}\right)^{-2/3} T_\odot^{-1/3} M^{2/3} m_2^{-1}.$$

$$T_{sun} = \frac{GM_{sun}}{c} = 4.925490947\,\mu s$$

$$s = \sin i$$

$$x \equiv a_p \sin i / c$$

$$M = m_1 + m_2$$

$$(m_1 = m_p; m_2 = m_{comp}) in M_{sun}$$

Post Keplerian (PK) parameter

If any two of these PK parameters are measured, the masses of the pulsar and its companion can be determined. If more than two are measured, each additional PK parameter yields a different test of a gravitational theory.

J0737-3039A (22.7 ms) & B (2.8 s) [Burgay + 2003]

After 12 months of observations timing measurements for A already provide five PK parameters.
Shaded regions are those excluded by the K mass functions of the two pulsars.
Further constrains (pair of lines) are predicted by GR.

$$m_A + m_B = 2.59 M_\odot$$

$$i = 88 \pm 1^0$$

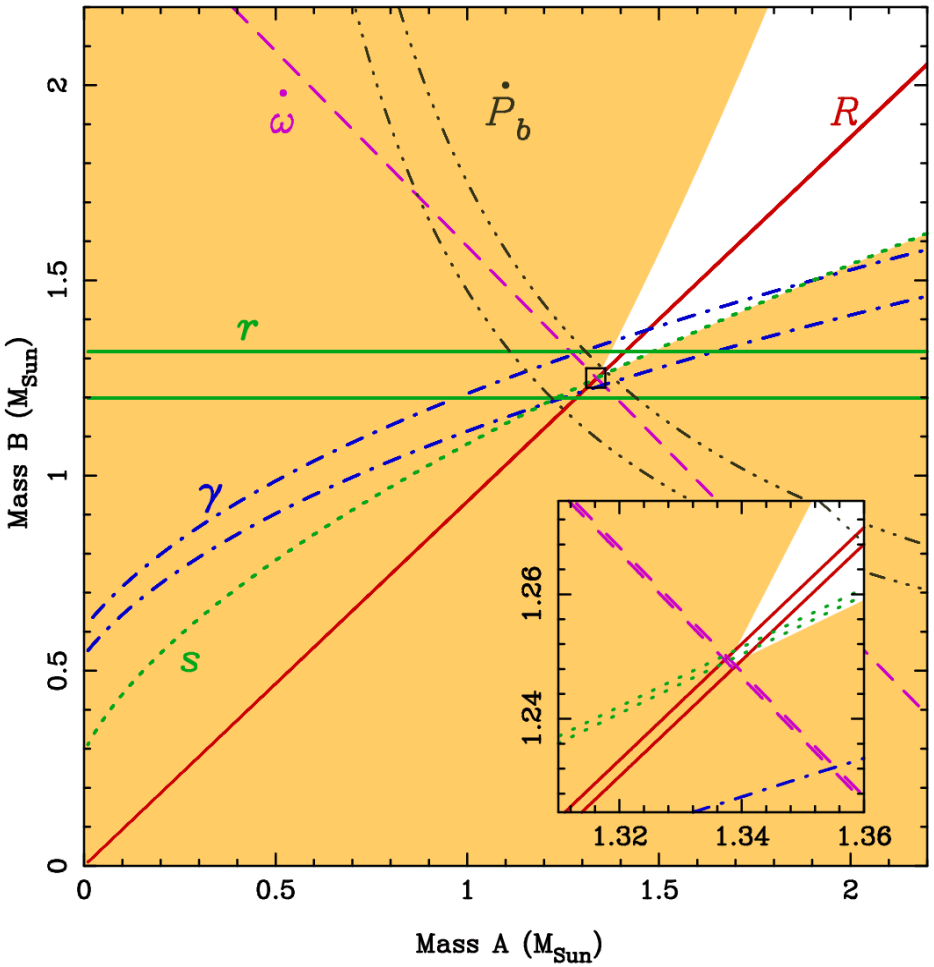

masses of the binary system J0737-3039A&B

The most massive Neutron Star yet known

- This pulsar, called PSR J1614-2230, spins 317 times per second, and the companion completes an orbit in just under nine days. The pair, some 3,000 light-years distant, are in an orbit seen almost exactly edge-on from Earth. That orientation was the key to making the mass measurement trough the Shapiro Delay (Ransom et al. 2010)

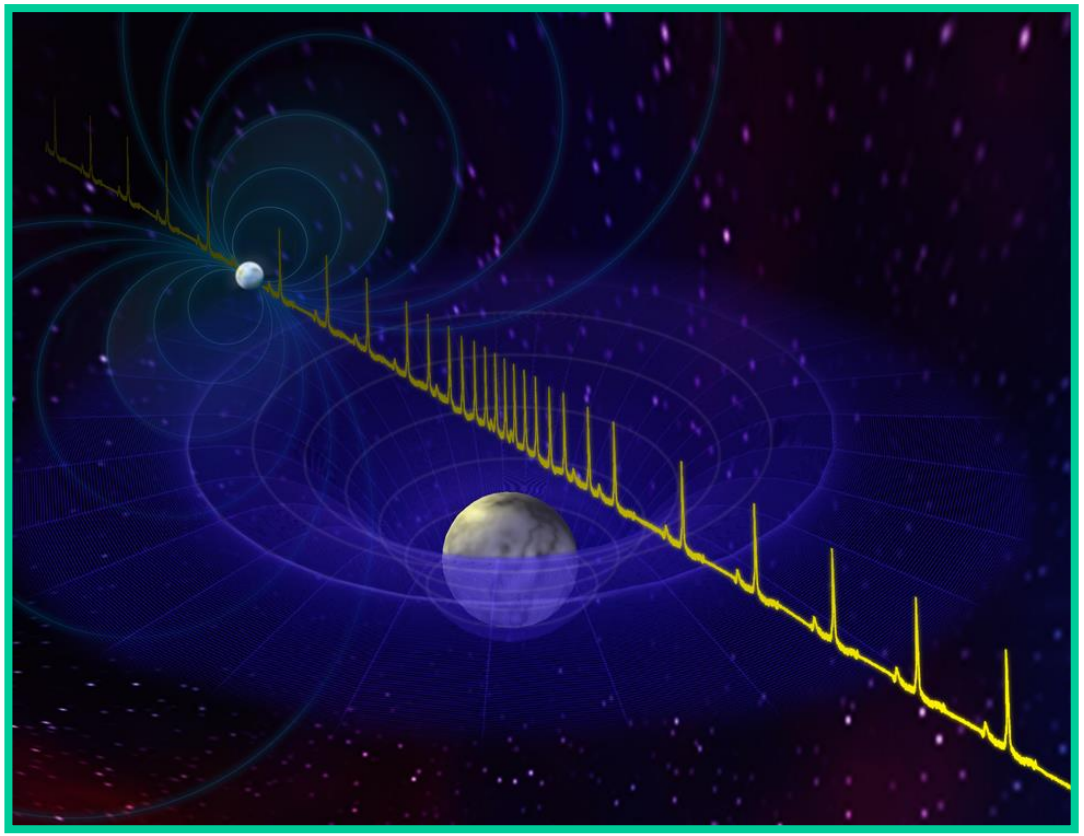

Pulses from neutron star (rear) are slowed as they pass near foreground white dwarf. This effect allowed astronomers to measure masses of the system. Credit: B. Saxton, NRAO/AUI/NSF

Neutron Stars and Pulsars

references/textbooks

M. Camenzind – **Compact Objects in Astrophysics** – A&A Library, Springer (cap. 5)
D.Lorimer & M. Kramer – **Handbook of Pulsar Astronomy** – COHRA , vol.4

Liebert, 1980, ARA&A, vol. 18, p. 363-398
Weidemann V. 1990, ARA&A, vol. 28, p. 103-137
D'Antona F., Mazzitelli I., A 1990, ARA&A, vol. 28, p.139-181
Hansen B.M.S, Liebert J. 2003, ARA&A, vol. 41, p. 465-515
Kramer M., Stairs I.H. 2008, ARA&A, vol 46, p.541-572

Neutron Star

Crab Nebula

M~1 Msol Massa

Radius ~ 10-15 km

Very strong magnetic field

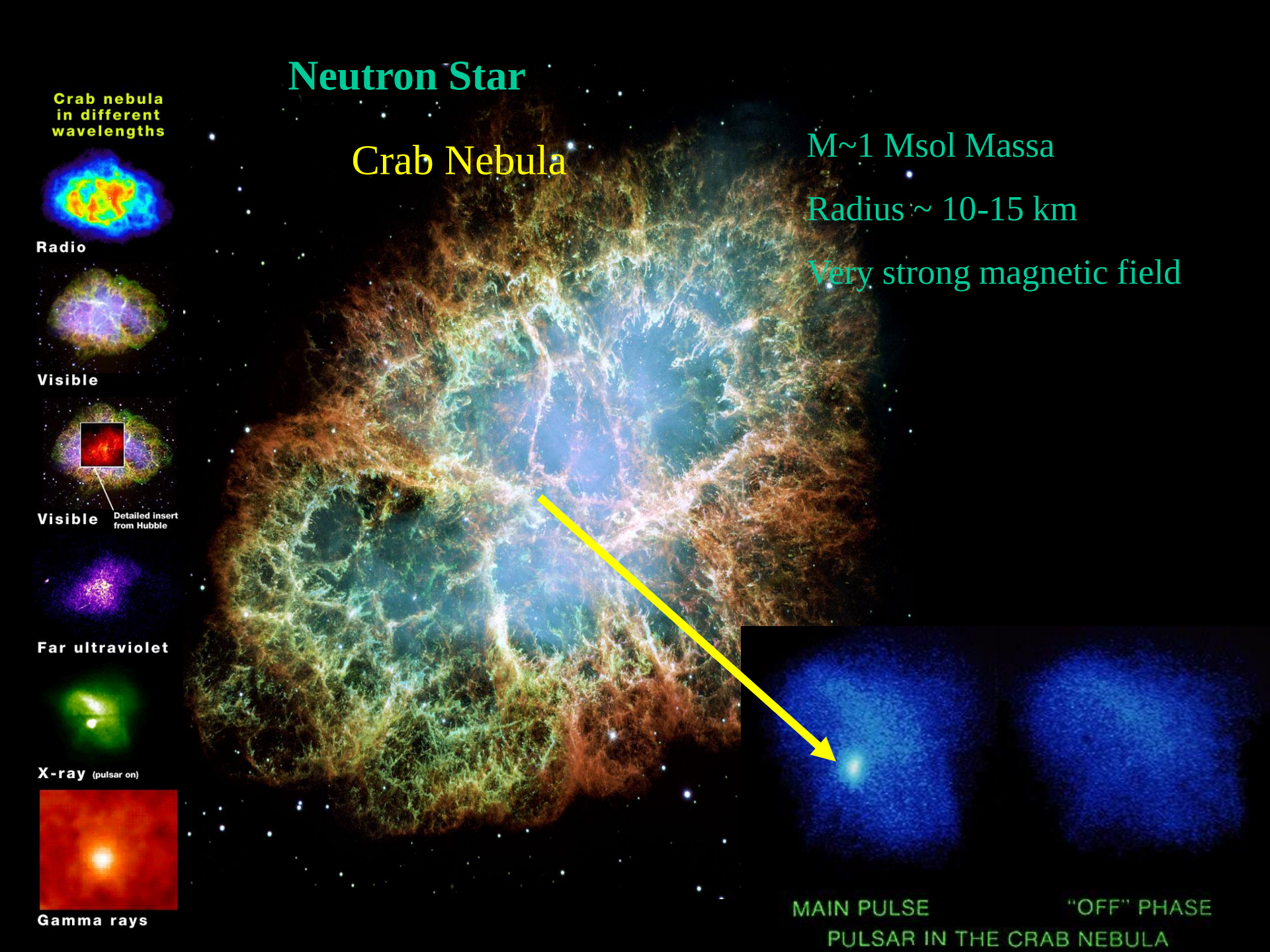

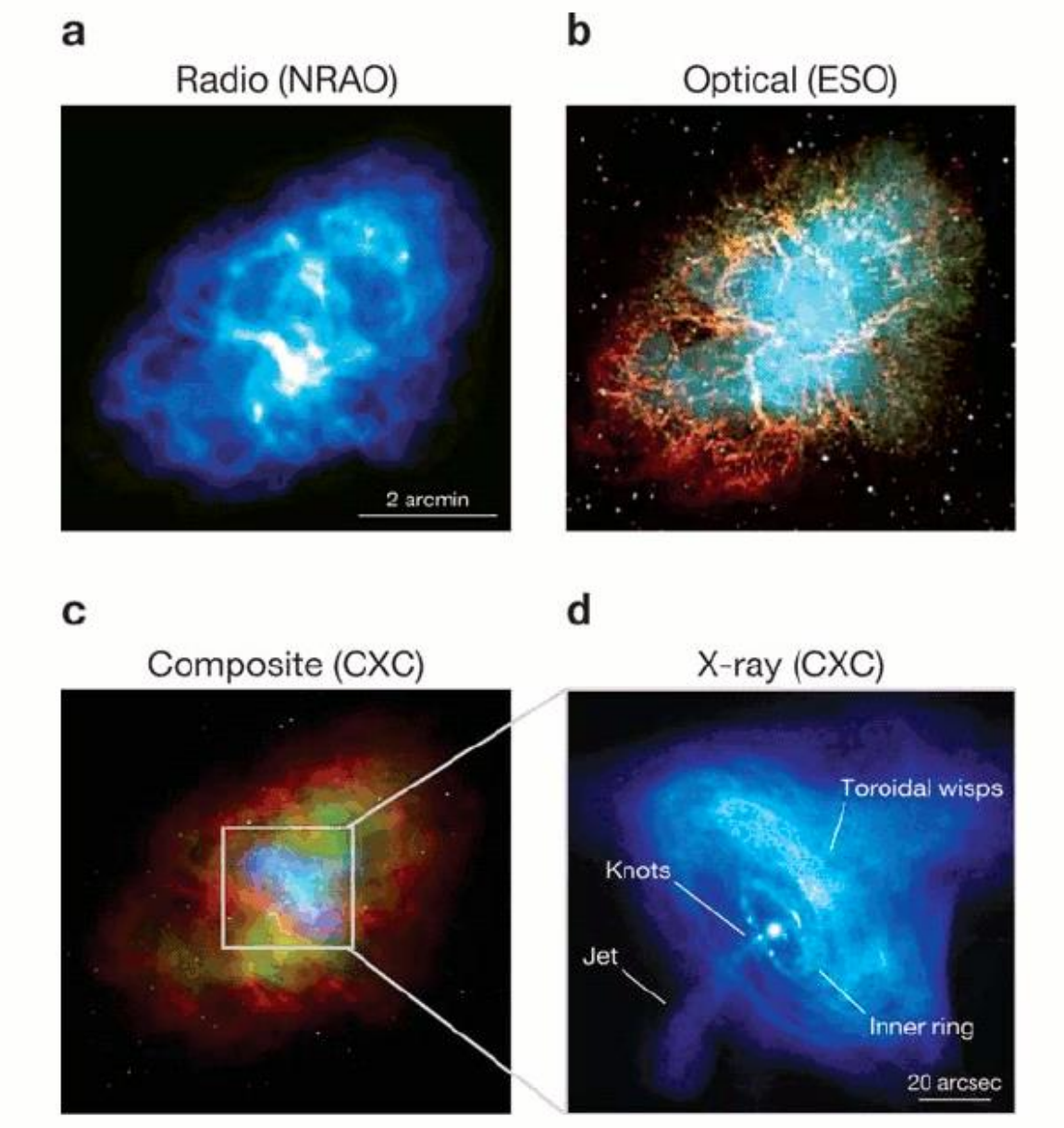
a
Radio (NRAO)
2 arcmin
b
Optical (ESO)
c
Composite (CXC)
d
X-ray (CXC)
Toroidal wisps
Knots
Jet
Inner ring
20 arcsec